Max-Planck-Institut für Mathematik in den Naturwissenschaften Leipzig

Geometry of Quantum Coherence for Two Qubit X States

by

Yao-Kun Wang, Lian-He Shao, Shao-Ming Fei, and Zhi-Xi Wang

Preprint no.: 69 2019

Geometry of Quantum Coherence for Two Qubit X States

Yao-Kun Wang,[1,2] Lian-He Shao,[3] Shao-Ming Fei,[4,5] and Zhi-Xi Wang[4]

[1] *College of Mathematics, Tonghua Normal University, Tonghua, Jilin 134001, China*
[2] *Research Center for Mathematics, College of Mathematics, Tonghua Normal University, Tonghua, Jilin 134001, China*
[3] *State and Local Joint Engineering Research Center for Advanced Networking and Intelligent Information Services, School of Computer Science, Xi'an Polytechnic University, Xi'an, 710048, Shaanxi, China*
[4] *School of Mathematical Sciences, Capital Normal University, Beijing 100048, China*
[5] *Max-Planck Institute for Mathematics in the Sciences, 04103 Leipzig, Germany*

We investigate the geometry with respect to several distance-based quantifiers of coherence for Bell-diagonal states. We find that as both l_1 norm and relative entropy of coherence vary continuously from zero to one, their related geometric surfaces move from the region of separable states to the region of entangled states, a fact illustrating intuitively that quantum states with nonzero coherence can be used for entanglement creation. We find the necessary and sufficient conditions that quantum discord of Bell-diagonal states equals to its relative entropy of coherence, and depict the surfaces related to the equality. We give surfaces of relative entropy of coherence for X states. We show the surfaces of dynamics of relative entropy of coherence for Bell-diagonal states under local nondissipative channels and find that all coherences under local nondissipative channels decrease.

I. INTRODUCTION

Quantum coherence originates in the superposition of quantum states. As a physical resource[1–3] like quantum entanglement and other quantum correlations, quantum coherence is an essential ingredient in quantum information processing[4–6], quantum metrology[7–9], quantum optics[10–12], nanoscale thermodynamics[13–18] and quantum biology[19–23]. Recently, a rigorous framework to quantify coherence has been proposed[3]. And a number of quantum coherence measures, such as the l_1 norm of coherence[3], the relative entropy of coherence[3], trace norm of coherence[24], Tsallis relative α entropies[25] and Relative Rényi α monotones[26], have been presented. With these coherence measures, many properties of quantum coherence, such as the relations between quantum coherence and quantum correlations[27–31], the fact that the relative entropy of coherence decreases strictly for all nontrivial evolutions in the dynamics of coherence[32], the freezing phenomenon of coherence[32, 33], have been investigated.

The geometry of Bell-diagonal states, including the separable and classical subsets, can be depicted in three dimensions[34, 35]. Level surfaces of entanglement and nonclassical measures can be plotted directly in terms of such three-dimensional geometry. The complete structure of entanglement and nonclassicality can be explicitly displayed. It is more illuminating to use such pictures to explain how the measures of entanglement and nonclassicality change rather than the other way around[36]. A series of researches have been done toward the geometry of quantum correlations, such as the level surfaces of quantum discord for a class of two-qubit states[37], the geometry of one-way information deficit for a class of two-qubit states[38], the surfaces of constant quantum discord and super-quantum discord for Bell-diagonal state[39], the geometric illustration of Bell-diagonal states steerable by two projective measurements[40].

In this article, we calculate several distance-based quantifiers of coherence for Bell-diagonal states and study the associated geometry. We plot the geometry both for the l_1-norm of coherence and the relative entropy of coherence for Bell-diagonal states in separable and entangled regions. We present the surfaces that quantum discord equals to the relative entropy of coherence for Bell-diagonal states. We depict the geometry of relative entropy of coherence for X states. We show the geometry of dynamics of relative entropy of coherence for Bell-diagonal states under local nondissipative channels.

II. GEOMETRY OF SEVERAL DISTANCE-BASED QUANTIFIERS OF COHERENCE FOR BELL-DIAGONAL STATES

The two-qubit Bell-diagonal states can be expressed by

$$\rho = \frac{1}{4}(I \otimes I + \sum_{i=1}^{3} c_i \sigma_i \otimes \sigma_i), \tag{1}$$

where $\{\sigma_i\}_{i=1}^3$ are the standard Pauli matrices. In the computational basis $|00\rangle, |01\rangle, |10\rangle, |11\rangle$, one has

$$\rho = \frac{1}{4}\begin{pmatrix} 1+c_3 & 0 & 0 & c_1-c_2 \\ 0 & 1-c_3 & c_1+c_2 & 0 \\ 0 & c_1+c_2 & 1-c_3 & 0 \\ c_1-c_2 & 0 & 0 & 1+c_3 \end{pmatrix}, \tag{2}$$

where $c_1, c_2, c_3 \in [-1, 1]$.

We study the geometry of several distance-based quantifiers of coherence for Bell-diagonal states, such as l_1-norm of coherence C_{l_1}[3], trace distance of C_{tr}[24], relative entropy of coherence C_r[3]. As Bell-diagonal states are X states, one has $C_{l_1} = C_{tr}$[41]. By straightforward computation, we have

$$C_{l_1}(\rho) = \sum_{i \neq j} |\rho_{i,j}| = \frac{1}{2}(|c_1 - c_2| + |c_1 + c_2|), \tag{3}$$

and

$$\begin{aligned} C_r(\rho) &= S(\rho_{diag}) - S(\rho) \\ &= \frac{1}{4}(1 - c_1 - c_2 - c_3)\log\frac{1}{4}(1 - c_1 - c_2 - c_3) \\ &+ \frac{1}{4}(1 - c_1 + c_2 - c_3)\log\frac{1}{4}(1 - c_1 + c_2 - c_3) \\ &+ \frac{1}{4}(1 + c_1 - c_2 + c_3)\log\frac{1}{4}(1 + c_1 - c_2 + c_3) \\ &+ \frac{1}{4}(1 + c_1 + c_2 + c_3)\log\frac{1}{4}(1 + c_1 + c_2 + c_3) \\ &+ 2 - \frac{1+c_3}{2}\log(1+c_3) - \frac{1-c_3}{2}\log(1-c_3). \end{aligned} \tag{4}$$

The geometry with respect to the l_1-norm of coherence and the relative entropy of coherence are similar [see Fig. 1 and Fig. 2]. The orange tetrahedron is the set of valid Bell-diagonal states. The green octahedron is the set of separable Bell-diagonal states. There are four entangled regions outside octahedron[36]. The the tube-like level surfaces are along the Cartesian axes C_3. The tubes are cut off by the state tetrahedron at their ends. As coherence decreases, the tubes collapse to the Cartesian axes. The tube structure is obscured as the coherence increases. From Eq. (3) and Eq. (4), one sees that the vanishes if and only if $c_1 = c_2 = 0$, and the geometry of coherence is the Cartesian axes C_3 that is completely in the set of separable Bell-diagonal states (the green octahedron). For small coherence, the surfaces move to the entangled region [see Fig. 1(a) and Fig. 2(a)]. With the increasing coherence, the surfaces distribute in both separable and entangled regions [see Fig. 1(b) and Fig. 2(b)]. When the coherence approaches 1, the surfaces almost distribute in the entangled regions [see Fig 1(c). and Fig. 2(c)]. When the coherence equals to 1, the surfaces lie in the four vertexes of the tetrahedron, which are four Bell states.

It can be also shown that the geometry related to the Tsallis α divergence [25] and Relative Rényi α monotones [26] for $\alpha = 1/2, 3/2, 2$ is extremely similar to the geometry of relative entropy of coherence.

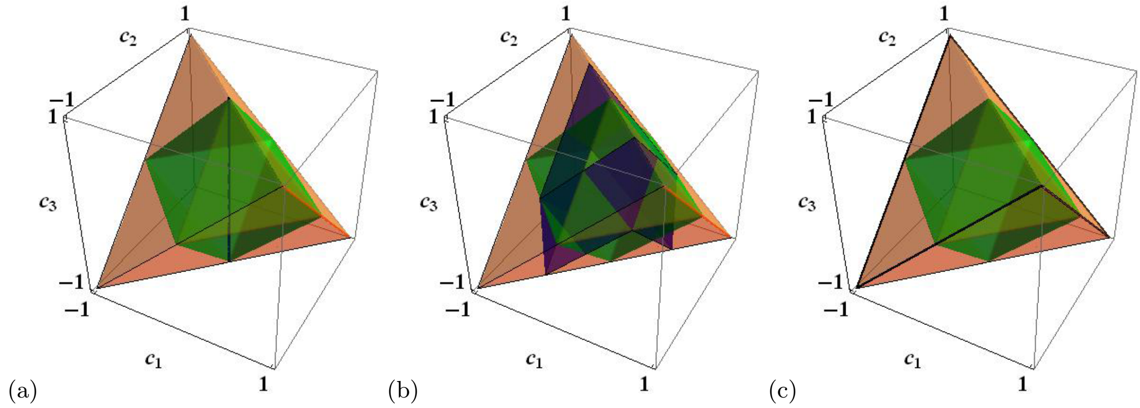

FIG. 1: Surfaces of constant l_1-norm of coherence C_{l_1} for Bell-diagonal states (Blue surfaces): (a) $C_{l_1} = 0.001$; (b) $C_{l_1} = 0.5$; (c) $C_{l_1} = 0.99$.

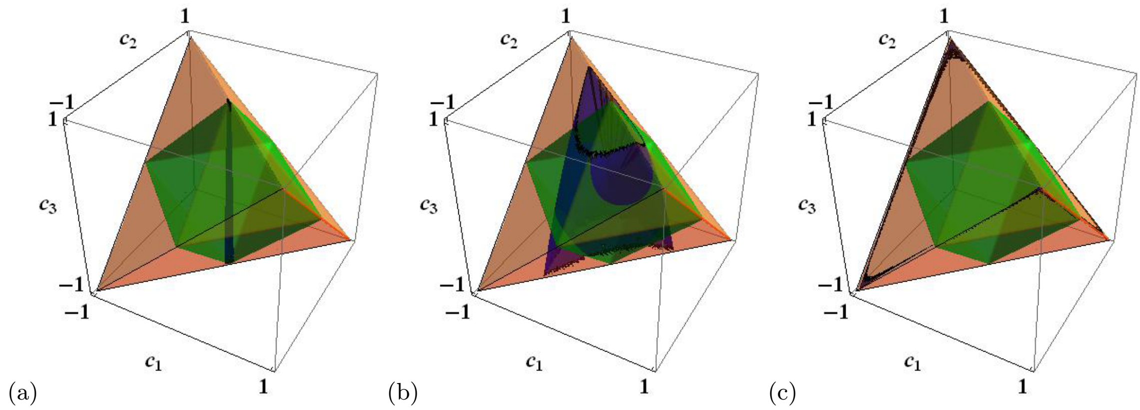

FIG. 2: Surfaces of constant relative entropy of coherence for Bell-diagonal states (Blue surfaces): (a) $C_r(\rho) = 0.001$; (b) $C_r(\rho) = 0.2$; (c) $C_r(\rho) = 0.9$.

We now investigate the surfaces that the quantum discord is equal to the relative entropy of coherence for Bell-diagonal states. The quantum discord $D(\rho)$ of Bell-diagonal states is given by[42],

$$\begin{aligned} D(\rho) \;=\; & \frac{1}{4}(1-c_1-c_2-c_3)\log\frac{1}{4}(1-c_1-c_2-c_3) \\ & +\frac{1}{4}(1-c_1+c_2-c_3)\log\frac{1}{4}(1-c_1+c_2-c_3) \\ & +\frac{1}{4}(1+c_1-c_2+c_3)\log\frac{1}{4}(1+c_1-c_2+c_3) \\ & +\frac{1}{4}(1+c_1+c_2+c_3)\log\frac{1}{4}(1+c_1+c_2+c_3) \\ & +2-\frac{1+c}{2}\log(1+c)-\frac{1-c}{2}\log(1-c), \end{aligned}$$

where $c = max\{|c_1|, |c_2|, |c_3|\}$. Comparing $D(\rho)$ with Eq. (4), we have that the quantum discord equal to relative entropy of coherence for Bell-diagonal states if and only if $c_3 = max\{|c_1|, |c_2|, |c_3|\}$. In Fig. 3 two blue tubes above and below the orange cross tube represent the surfaces of $C_r(\rho) = D(\rho) = 0.05$.

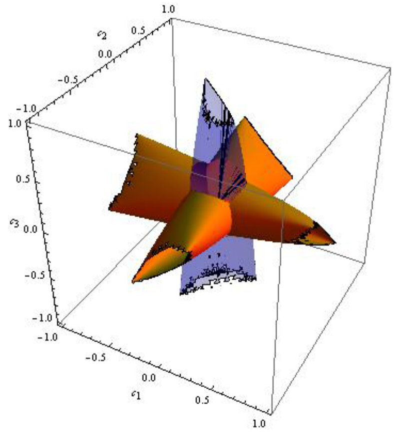

FIG. 3: (Color online) Surfaces of $C_r(\rho) = D(\rho) = 0.05$ for Bell-diagonal states (two Blue tubes).

III. GEOMETRY OF RELATIVE ENTROPY OF COHERENCE FOR X STATES

We consider now general two qubit X states. Under proper local unitary transformations, the two qubit X states can be written as,

$$\rho = \frac{1}{4}(I \otimes I + \mathbf{r} \cdot \sigma \otimes I + I \otimes \mathbf{s} \cdot \sigma + \sum_{i=1}^{3} c_i \sigma_i \otimes \sigma_i), \tag{5}$$

where $\mathbf{r}$ and $\mathbf{s}$ are Bloch vectors. When $\mathbf{r}$=$\mathbf{s}$=$\mathbf{0}$, ρ reduces to the two-qubit Bell-diagonal states. We assume that the Bloch vectors are in z direction, $\mathbf{r} = (0, 0, r)$, $\mathbf{s} = (0, 0, s)$. The state in Eq. (5) turns into the following form

$$\rho = \frac{1}{4}(I \otimes I + r\sigma_3 \otimes I + I \otimes s\sigma_3 + \sum_{i=1}^{3} c_i \sigma_i \otimes \sigma_i).$$

In the computational basis $|00\rangle, |01\rangle, |10\rangle, |11\rangle$, one has

$$\rho = \frac{1}{4}\begin{pmatrix} 1+r+s+c_3 & 0 & 0 & c_1-c_2 \\ 0 & 1+r-s-c_3 & c_1+c_2 & 0 \\ 0 & c_1+c_2 & 1-r+s-c_3 & 0 \\ c_1-c_2 & 0 & 0 & 1-r-s+c_3 \end{pmatrix}. \tag{6}$$

From the Eq. (4) in [43], after some algebraic calculations, we have the relative entropy of coherence for X states,

$$\begin{aligned} C_r(\rho) &= S(\rho_{diag}) - S(\rho) \\ &= \frac{1}{4}(1-c_3+\sqrt{(r-s)^2+(c_1+c_2)^2})\log(1-c_3+\sqrt{(r-s)^2+(c_1+c_2)^2}) \\ &\quad +\frac{1}{4}(1-c_3-\sqrt{(r-s)^2+(c_1+c_2)^2})\log(1-c_3-\sqrt{(r-s)^2+(c_1+c_2)^2}) \\ &\quad +\frac{1}{4}(1+c_3+\sqrt{(r+s)^2+(c_1-c_2)^2})\log(1+c_3+\sqrt{(r+s)^2+(c_1+c_2)^2}) \\ &\quad +\frac{1}{4}(1+c_3-\sqrt{(r+s)^2+(c_1-c_2)^2})\log(1+c_3-\sqrt{(r+s)^2+(c_1-c_2)^2}) \\ &\quad -\frac{1}{4}(1+r+s+c_3)\log(1+r+s+c_3) \\ &\quad -\frac{1}{4}(1+r-s-c_3)\log(1+r-s-c_3) \\ &\quad -\frac{1}{4}(1-r+s-c_3)\log(1-r+s-c_3) \\ &\quad -\frac{1}{4}(1-r-s+c_3)\log(1-r-s+c_3). \end{aligned} \tag{7}$$

In Fig. 4 we plot the surface of relative entropy of coherence for X states. From Fig. 4, one can see that the level surface of coherence is similar to the case $r = s = 0$, i.e., the one of Bell-diagonal states [see Fig. 4(a)]. The surface shrinks with the increasing r and s. The shrinking rate becomes larger with the increasing $|r|$ and $|s|$ [see Fig. 4(a), (b)]. For larger r and s, the picture is moved up to the plane $c_3 = 0$ [see Fig. 4(b)]. For larger coherence and small r and s [see Fig. 4(c)], the surface becomes fat and short. But for larger r and s [see Fig. 4(d)], the figure is moved up again and changes dramatically too.

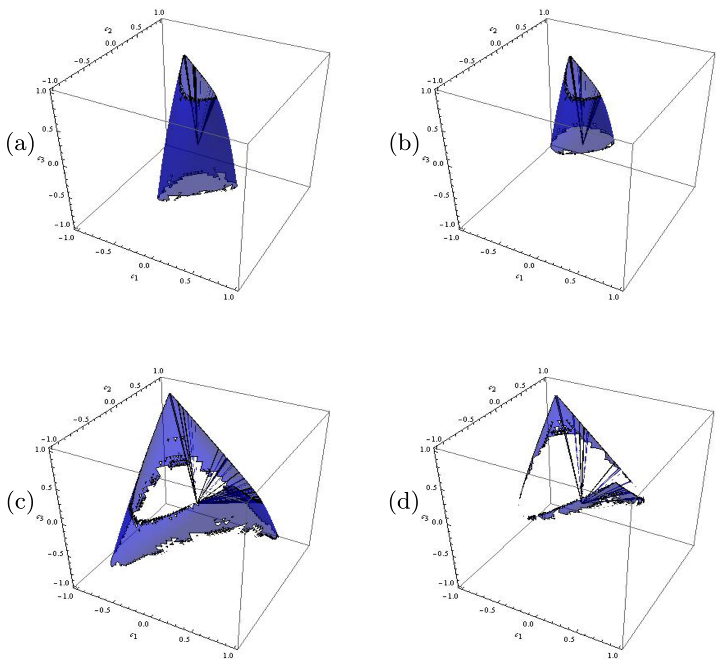

FIG. 4: (Color online) Surfaces of constant relative entropy of coherence for X states(blue surface): (a)$r = s = 0.1, C_r = 0.1$; (b)$r = s = 0.5, C_r = 0.1$; (c)$r = s = 0.1, C_r = 0.5$; (d)$r = s = 0.5, C_r = 0.5$.

	Kraus operators
BF	$E_0 = \sqrt{1-p/2}\, I, \quad E_1 = \sqrt{p/2}\, \sigma_1$
PF	$E_0 = \sqrt{1-p/2}\, I, \quad E_1 = \sqrt{p/2}\, \sigma_3$
BPF	$E_0 = \sqrt{1-p/2}\, I, \quad E_1 = \sqrt{p/2}\, \sigma_2$
GAD	$E_0 = \sqrt{p}\begin{pmatrix} 1 & 0 \\ 0 & \sqrt{1-\gamma} \end{pmatrix}, \quad E_2 = \sqrt{1-p}\begin{pmatrix} \sqrt{1-\gamma} & 0 \\ 0 & 1 \end{pmatrix}$
	$E_1 = \sqrt{p}\begin{pmatrix} 0 & \sqrt{\gamma} \\ 0 & 0 \end{pmatrix}, \quad E_3 = \sqrt{1-p}\begin{pmatrix} 0 & 0 \\ \sqrt{\gamma} & 0 \end{pmatrix}$

TABLE I: Kraus operators for the quantum channels: bit flip (BF), phase flip (PF), bit-phase flip (BPF), and generalized amplitude damping (GAD), where p and γ are decoherence probabilities, $0 < p < 1$, $0 < \gamma < 1$.

Channel	c'_1	c'_2	c'_3
BF	c_1	$c_2(1-p)^2$	$c_3(1-p)^2$
PF	$c_1(1-p)^2$	$c_2(1-p)^2$	c_3
BPF	$c_1(1-p)^2$	c_2	$c_3(1-p)^2$
GAD	$c_1(1-p)$	$c_2(1-p)$	$c_3(1-p)^2$

TABLE II: Correlation coefficients with respect to: bit flip (BF), phase flip (PF), bit-phase flip (BPF), and generalized amplitude damping (GAD). For GAD, we fixed $p = 1/2$ and replaced γ by p.

IV. GEOMETRY OF DYNAMICS OF RELATIVE ENTROPY OF COHERENCE FOR BELL-DIAGONAL STATES UNDER LOCAL NONDISSIPATIVE CHANNELS

We consider next the system-environment interaction[44] by the evolution of a quantum state ρ under a trace-preserving quantum operation $\varepsilon(\rho)$,

$$\varepsilon(\rho) = \sum_{i,j} (E_i \otimes E_j)\, \rho\, (E_i \otimes E_j)^\dagger ,$$

where $\{E_k\}$ is the set of Kraus operators associated to a decohering process of a single qubit, with $\sum_k E_k^\dagger E_k = I$. We use the Kraus operators in Table I [45] for a variety of quantum channels.

The decoherence processes BF, PF, and BPF in Table I preserve the Bell-diagonal form of the density operator ρ_{AB}. For the case of GAD, the Bell-diagonal form is kept for arbitrary γ and $p = 1/2$. In this situation, we can write the quantum operation $\varepsilon(\rho)$ as

$$\varepsilon(\rho_{AB}) = \frac{1}{4}(I \otimes I + \sum_{i=1}^{3} c'_i \sigma_i \otimes \sigma_i),$$

where the values of the c'_1, c'_2, c'_3 are given in Table II [45].

Replacing c_i by c_i' in Eq. (4), we plot the surfaces of the relative entropy of coherence for Bell-diagonal states under local nondissipative channels. one can see that when the relative entropy of coherence increases, the surfaces of coherence become fat [see (a), (b) of Figs. 5, 6, 7, 8]. Furthermore, when p increases, the surfaces of coherence under BF and BPF become two opposite surfaces [see (c) of Figs. 5, 7]. And the surface of coherence under PF becomes four small triangle surfaces [Fig. 6(c)]. While the surface of coherence under GAD becomes a cylinder [see Fig. 8(c)].

On the other hand, for $c_1 = -0.1, c_2 = 0.4, c_3 = 0.4$ and $c_1 = -0.5, c_2 = 0.1, c_3 = 0.1$, the dynamic behavior of relative entropy of coherence of Bell-diagonal states under bit flip, phase flip, bit-phase flip, and generalized amplitude damping channels is depicted in Fig. 9. We find that C_{pf} and C_{gad} approach zero as p increases, and all the coherences under local nondissipative channels decrease. It is a special case of the relative entropy of coherence which decreases strictly for all nontrivial evolutions[32]. Although C_{bf} decreases as p increases in Fig. 9(a), it keeps almost unchanged in Fig. 9(b), similar to freezing phenomenon of coherence[32, 33].

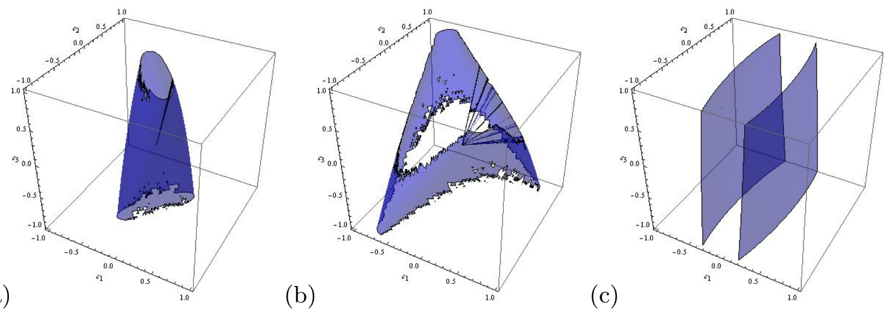

(a) (b) (c)

FIG. 5: Surfaces of relative entropy of coherence for Bell-diagonal states under bit flip channels:(a) $p = 0.1, C_r(\rho) = 0.1$; (b) $p = 0.1, C_r(\rho) = 0.5$; (c) $p = 0.5, C_r(\rho) = 0.1$.

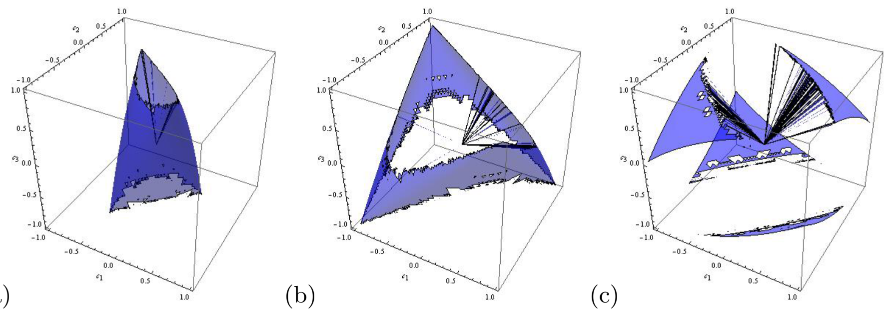

(a) (b) (c)

FIG. 6: Surfaces of relative entropy of coherence for Bell-diagonal states under phase flip channels:(a) $p = 0.1, C_r(\rho) = 0.1$; (b) $p = 0.1, C_r(\rho) = 0.5$; (c) $p = 0.5, C_r(\rho) = 0.1$.

V. SUMMARY

We have calculated several distance-based quantifiers of coherence for Bell-diagonal states including l_1-norm of coherence and relative entropy of coherence, and illustrated the corresponding geometries. The geometry associated with the l_1-norm of coherence and the relative entropy of coherence are basically the

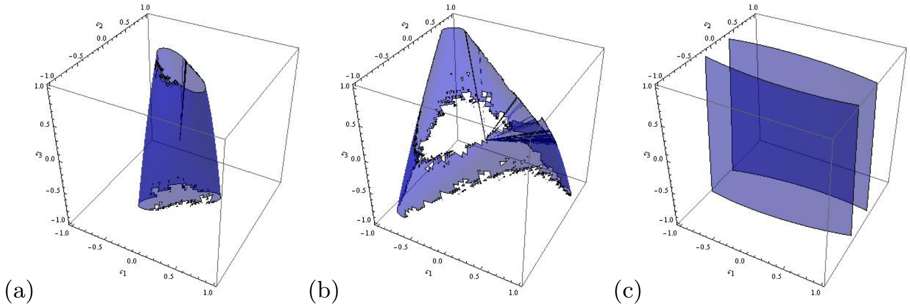

FIG. 7: Surfaces of relative entropy of coherence for Bell-diagonal states under bit-phase flip channels:(a) $p = 0.1, C_r(\rho) = 0.1$; (b) $p = 0.1, C_r(\rho) = 0.5$; (c) $p = 0.5, C_r(\rho) = 0.1$.

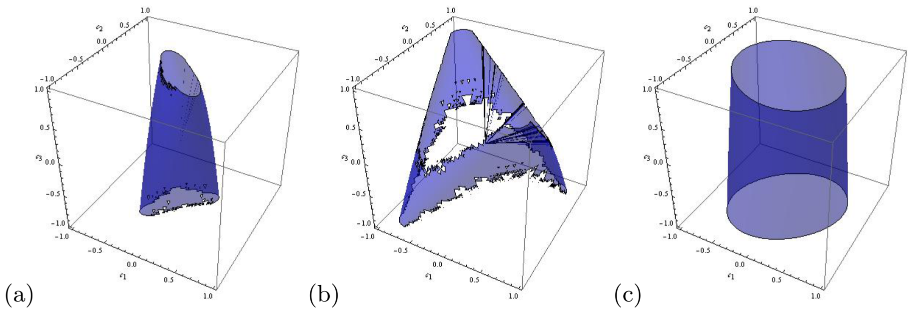

FIG. 8: Surfaces of relative entropy of coherence for Bell-diagonal states under generalized amplitude damping channels:(a) $p = 0.1, C_r(\rho) = 0.1$; (b) $p = 0.1, C_r(\rho) = 0.5$; (c) $p = 0.5, C_r(\rho) = 0.1$.

same except for the shape of the parallelogram. The level surfaces consist of tubes along the Cartesian axes C_3. These tubes are cut off by the state tetrahedron at their ends. As the coherence decreases, the tubes collapse to the Cartesian axes C_3. Such tube structure becomes obscured as the coherence increases. It has been shown that when the coherence approaches zero, the geometry of coherence is the Cartesian axes C_3 that lies completely in the set of separable Bell-diagonal states. For small coherence, the surfaces move to the entangled region. As coherence increases, the surfaces distribute both in separable and entangled regions. When the coherence approaches 1, the surfaces almost distribute in the entangled regions. When the coherence is equal to 1, the surfaces are the four vertexes of the tetrahedron with respect to the four Bell states.

We have shown that the quantum discord equals to the relative entropy of coherence for Bell-diagonal states if and only if $c_3 = max\{|c_1|, |c_2|, |c_3|\}$. The related surfaces of for the equality has been plotted.

We have also plotted the surfaces of relative entropy of coherence for X states, showing that the surface shrinks with the increasing r and s, and the shrinking rate becomes larger with the increasing $|r|$ and $|s|$. For larger r and s, the surfaces move up the plane $c_3 = 0$. For larger coherence and small r and s, the surfaces become fat and short.

The surfaces of dynamics with respect to the relative entropy of coherence for Bell-diagonal states under local nondissipative channels have been also studied. We have shown that when the relative entropy of coherence increases, the surfaces of coherence become fat. What is more, when p increases, the surfaces of coherence under bit flip and bit-phase flip channels become two opposite surfaces, the surface of coherence

(a) (b)

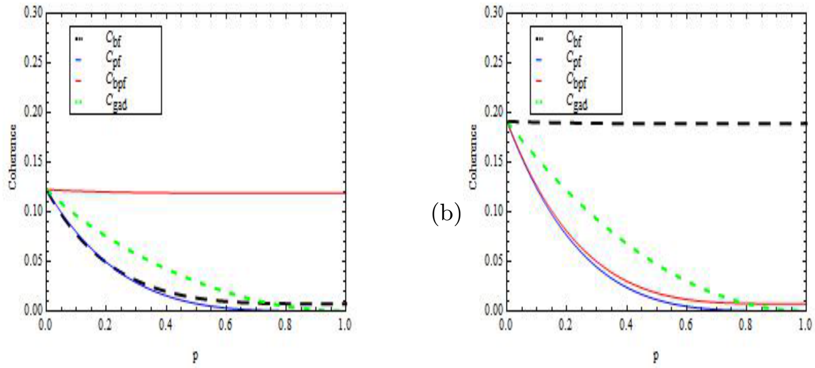

FIG. 9: (Color online) Relative entropy of coherence C_{bf}, C_{pf}, C_{bpf} and C_{gad} for Bell-diagonal states under bit flip, phase flip, bit-phase flip and generalized amplitude damping channels as a function of p, respectively: (a) $c_1 = -0.1, c_2 = 0.4, c_3 = 0.4$; (b) $c_1 = -0.5, c_2 = 0.1, c_3 = 0.1$.

under phase flip channel becomes four small triangle surfaces, and the surface of coherence under generalized amplitude damping channel becomes a cylinder.

We have also studied the dynamic behavior of relative entropy of coherence of Bell-diagonal states. It has been shown that all the coherence under local nondissipative channels decreases, and the coherences under phase flip channel and generalized amplitude damping channel approach zero as p increases.

Acknowledgments We thank Q. Quan and T. Ma for useful discussions. This work was supported by the National Natural Science Foundation of China under grant Nos. ???? 11675113 and NSF of Beijing under No. KZ201810028042.

[1] T. Sashki, Y. Yamamoto, and M. Koashi, Nature (London) **509**, 475 (2014).
[2] J. Aberg, Phys. Rev. Lett. **113**, 150402 (2014).
[3] T. Baumgratz, M. Cramer, and M. B. Plenio, Phys. Rev. Lett. **113**, 140401 (2014).
[4] E. Bagan, J. A. Bergou, S. S. Cottrell, and M. Hillery, Phys. Rev. Lett. **116**, 160406 (2016).
[5] P. K. Jha, M. Mrejen, J. Kim, C. Wu, Y. Wang, Y. V. Rostovtsev, and X. Zhang, Phys. Rev. Lett. **116**, 165502 (2016).
[6] P. Kammerlander and J. Anders, Sci. Rep. **6**, 22174 (2016).
[7] V. Giovannetti, S. Lloyd, and L. Maccone, Science **306**, 1330 (2004).
[8] R. Demkowicz-Dobrzański and L. Maccone, Phys. Rev. Lett. **113**, 250801 (2014).
[9] V. Giovannetti, S. Lloyd, and L. Maccone, Nat. Photonics **5**, 222 (2011).
[10] R. J. Glauber, Phys. Rev. **131**, 2766 (1963).
[11] E. C. G. Sudarshan, Phys. Rev. Lett. **10**, 277 (1963).
[12] L. Mandel and E. Wolf, *Optical Coherence and Quantum Optics* (Cambridge University Press, Cambridge, UK, 1995).
[13] V. Narasimhachar and G. Gour, Nat. Commun. **6**, 7689 (2015).
[14] P. Ćwikliński, M. Studziński, M. Horodecki, and J. Oppenheim, Phys. Rev. Lett. **115**, 210403 (2015).
[15] M. Lostaglio, D. Jennings, and T. Rudolph, Nat. Commun. **6**, 6383 (2015).
[16] M. Lostaglio, K. Korzekwa, D. Jennings, and T. Rudolph, Phys. Rev. X **5**, 021001 (2015).
[17] H. Vazquez, R. Skouta, S. Schneebeli, M. Kamenetska, R. Breslow, L. Venkataraman, and M. S. Hybertsen, Nat. Nanotechnol. **7**, 663 (2012).
[18] O. Karlström, H. Linke, G. Karlström, and A. Wacker, Phys. Rev. B **84**, 113415 (2011).
[19] M. B. Plenio and S. F. Huelga, New J. Phys. **10**, 113019 (2008).
[20] P. Rebentrost, M. Mohseni, and A. Aspuru-Guzik, J. Phys. Chem. B **113**, 9942 (2009).
[21] S. Lloyd, J. Phys: Conf. Ser. **302**, 012037 (2011).
[22] C.-M. Li, N. Lambert, Y.-N. Chen, G.-Y. Chen, and F. Nori, Sci. Rep. **2**, 885 (2012).
[23] S. F. Huelga and M. B. Plenio, Contemp. Phys. **54**, 181 (2013).

[24] L.-H. Shao, Z. Xi, H. Fan and Y. Li, Phys. Rev. A **91** 042120 (2015).
[25] A. E. Rastegin, Phys. Rev. A **93** 032136 (2016).
[26] E. Chitambar and G. Gour, Phys. Rev. A **94** 052336 (2016).
[27] J. Ma, B. Yadin, D. Girolami, V. Vedral, and M. Gu, Phys. Rev. Lett. **116**, 160407 (2016).
[28] C. Radhakrishnan, M. Parthasarathy, S. Jambulingam, and T. Byrnes, Phys. Rev. Lett. **116**, 150504 (2016).
[29] A. Streltsov, U. Singh, H. S. Dhar, M. N. Bera, and G. Adesso, Phys. Rev. Lett. **115**, 020403 (2015).
[30] Y. Yao, X. Xiao, L. Ge, and C. P. Sun, Phys. Rev. A **92**, 022112 (2015).
[31] Z. Xi, Y. Li, and H. Fan, Sci. Rep. **5**, 10922 (2015).
[32] T. R. Bromley, M. Cianciaruso, and G. Adesso, Phys. Rev. Lett. **114**, 210401 (2015).
[33] X.-D. Yu, D.-J. Zhang, C. L. Liu, and D. M. Tong, Phys. Rev. A **93**, 060303 (2016).
[34] R. Horodecki, P. Horodecki, M. Horodecki, and K. Horodecki, Rev. Mod. Phys. **81**, 865 (2009), and references therein.
[35] R. Horodecki and M. Horodecki, Phys. Rev. A **54**, 1838 (1996).
[36] M. D. Lang and C. M. Caves, Phys. Rev. Lett. **105**, 150501 (2010).
[37] B. Li, Z.-X. Wang, and S.-M. Fei, Phys. Rev. A **83**, 022321 (2011).
[38] Y.-K. Wang, T. Ma, B. Li, Z.-X. Wang, Commun. Theor. Phys. **59**, 540 (2013).
[39] Y.-K. Wang, T. Ma, H. Fan, S.-M. Fei, Z.-X. Wang, Quantum Inf Process **13**, 283 (2014).
[40] Q. Quan, H. Zhu, S.-Y. Liu, S.-M. Fei, H. Fan, and W.-L. Yang, Sci. Rep. **6**, 22025 (2016).
[41] S. Rana, P. Parashar, and M. Lewenstein, Phys. Rev. A **93**, 012110 (2016).
[42] S. Luo, Phys. Rev. A **77**, 042303 (2008).
[43] Q. Chen, C. Zhang, S. Yu, X. X. Yi, and C. H. Oh, Phys. Rev. A **84**, 042313 (2011).
[44] M. A. Nielsen, and I. L. Chuang, *Quantum Computation and Quantum Information* (Cambridge University Press, Cambridge, UK, 2000).
[45] J. D. Montealegre, F. M. Paula, A. Saguia, and M. S Sarandy, Phys. Rev. A **87**, 042115 (2013).